Preparation and Crystal Structures of New Colorless 4-Amino-1-methylpyridinium Benzenesulfonate Salts for Second-Order Nonlinear Optics

Anwar, Shuji Okada, Hidetoshi Oikawa, and Hachiro Nakanishi*

Institute for Chemical Reaction Science, Tohoku University, 2-1-1 Katahira, Aoba-ku, Sendai 980-8577, Japan

A series of ionic 4-amino-1-methylpyridinium benzenesulfonate salts have been prepared by quaternization reaction of 4-aminopyridine with methyl benzenesulfonates having a substituent of hydroxy, methoxy, methyl, chloro, or bromo group at para position. The X-ray structure analysis has been performed for their single crystals which were obtained by slow evaporation of their methanol solutions. The salts were found to crystallize into noncentrosymmetric structures; triclinic space group $P1$ for the hydroxy derivative, monoclinic space group $P2_1$ for the methoxy and methyl derivatives, and monoclinic space group Cc for the chloro and bromo derivatives. By using the molecular structures and the molecular first hyperpolarizability (β) of the corresponding cation and anions, the components of second-harmonic tensor coefficient d of the crystals were evaluated by the oriented-gas model. The diagonal d components of the crystals were estimated to be as large as one-fourth of that of 2-methyl-4-nitroaniline (MNA) at 1064-nm laser wavelength irrespective of their very short absorption cutoff wavelength in the UV region. These colorless crystals could be a new series of prospective crystalline materials for second-order nonlinear optical applications using conventional diode lasers.

Introduction

From intensive research activity in the field of organic synthesis has emerged potential organic materials for second-order nonlinear optical (NLO) devices.[1,2] The main merits of organic materials compared with inorganic ones for such electrooptic modulation, frequency mixing and second-harmonic generation (SHG) devices are the large macroscopic second-order NLO susceptibilities ($\chi^{(2)}$), low dielectric constants, ultrafast optical response time, and high optical damage thresholds.[3] For obtaining the materials with large $\chi^{(2)}$, optimization of both the molecular first hyperpolarizability (β) and their orientation in the bulk are required. Organic molecules of large β, according to the useful guideline of two-level model,[4] should have a large difference in dipole moment of molecule between the ground state and excited state,

a large transition dipole moment, and a small band-gap energy. In synthesis, those are achieved by attaching strong donor and acceptor groups at the ends of the chromophores and/or elongation of the π-conjugated electron system. On the other hand, for bulk materials of large $\chi^{(2)}$, crystals of the organic chromophores with large β belonging to noncentrosymmetric space groups are one of the desired form. This is more preferred than other materials such as poled polymers[5] and self-assembled molecular layers,[6] since single crystals provide long-range orientational stability of acentric arrangements and the possibility of achieving a large $\chi^{(2)}$ tensor for certain applications.

However, only a few chromophores with large β have been developed into useful bulk crystalline materials for practical NLO applications. This is because the use of the classical nonionic chromophores is hampered by severe requirements; they often form crystals of centrosymmetric space groups which vanish all components of $\chi^{(2)}$, or although they achieve noncentrosymmetric structures, the orientation of their molecular dipole moments in the crystalline solid with respect to the polar crystal axes are not optimum for maximizing second-order NLO response.

(1) For reviews on organic materials for NLO, see: (a) *Nonlinear Optical Properties of Organic Molecules and Crystals*; Chemla, D. S., Zyss, J., Eds.; Academic Press: New York, 1987; Vols. 1 and 2. (b) *Introduction to Nonlinear Optical Effect in Molecules and Polymers*; Prasad, P. N., Williams, D. J., Eds.; A Wiley-Interscience Publ.: New York, 1990. (c) *Organic Materials for Nonlinear Optics II*; Hahn, R. A., Bloor, D., Eds.; Spec. Publ. No. 91; The Royal Society of Chemistry: London, 1989.
(2) For reviews on applications of organic NLO materials, see: (a) *Materials for Nonlinear Optics: Chemical Persepective*; Marder, S. R., Sohn, J. E., Stucky, J. D., Eds.; ACS Symp. Ser. 455; American Chemical Society: Washington, DC, 1991. (b) *Organic Materials for Nonlinear Optics III*; Ashwell, G. J., Bloor, D., Eds.; Spec. Publ. No.137; The Royal Society of Chemistry: London, 1993. (c) *Organic, Metalloorganic, and Polymeric Materials for Nonlinear Optical Appplications*; Marder, S. R., Perry, J. W., Eds.; Proc. SPIE Vol. 2134; The International Society for Optical Engineering: Washington, DC, 1994.
(3) *Molecular Nonlinear Optics: Materials, Physics, and Devices*; Zyss, J., Ed.; Academic Press: New York, 1994.
(4) Oudar J. L.; Chemla, D. S. *J. Chem. Phys.* **1977,** *66*, 2664.

(5) For discussions of poling experiments with polymer, see instance: (a) Hubbard, M. A.; Marks, T. J.; Yang, J. Y.; Wong, G. K. *Chem. Mater.* **1989,** *1*, 167. (b) Gilmour, S.; Montgomery, R. A.; Marder, S. R.; Cheng, L. T.; Jen, A. K.-Y.; Cai, Y.; Perry, J. W.; Dalton, L. R. *Chem. Mater.* **1994,** *6*, 1603.
(6) For discussions of self-assembly molecular layers, see: (a) Li, D.; Ratner, M. A.; Marks, T.; Zang, C.; Yang, J.; Wong, G. K. *J. Am Chem. Soc.* **1990,** *112*, 7389. (b) Katz, H. E.; Sheller, G.; Putvinski, T. M.; Schilling, M. L.; Wilson W. L.; Chidsey, C. E. D. *Science* **1991**, 254, 1485.

Following the work of Meredith,[7] our group[8–12] and Marder's group[13–18] have reported the strategy so-called salt methodology, i.e., the crystallization of ionic salts, to overcome the symmetry problem. This approach has been demonstrated to be a promising strategy for engineering the molecules into noncentrosymmetric alignment by virtue of complexation with a variety of counterions. For instance, variation of counteranions of stilbazolium cation species can develop a number of second-harmonic generation (SHG) active crystalline materials. Moreover, several of them have extremely large $\chi^{(2)}$, i.e., single crystals of stilbazoliums with *p*-toluenesulfonate (*p*TS) such as (*N*,*N*-dimethylamino) and hydroxy-substituted stilbazolium-*p*TS (DAST[9,14] and MC−PTS[10]). These two crystals have a second-order NLO susceptibility of more than 10 times higher than that of currently available inorganic materials such as LiNbO$_3$.[14]

The extremely large $\chi^{(2)}$ of those crystals are mainly provided by large β values of stilbazolium cations having the donor substituents. In general, the large β values of ionic species are due to strong electron acceptor and electron donor characteristics of the cation and anion parts, respectively. Therefore, any ionic π-conjugated compounds are highly polarized when a proper substituent is introduced at the opposite end of π-conjugation system to the ion part. In our previous study, we have reported that substituted stilbazolium cations possess β values of 2 orders larger than that of the standard *p*NA,[19] while that of *p*TS anion has a β value about equal to that of *p*NA.[20]

For frequency conversion devices of conventional diode lasers, however, the materials having short absorption cutoff (λ_{co}) wavelength in optical spectra, shorter than 400 nm, is required. This restricts the use of crystals of stilbazolium derivative and other colored compounds. To obtain colorless materials, we have investigated substituted pyridinium cations which are considered to shorten the π-conjugation of stilbazolium cations. Preparation of substituted pyridinium cations and their β values evaluated using
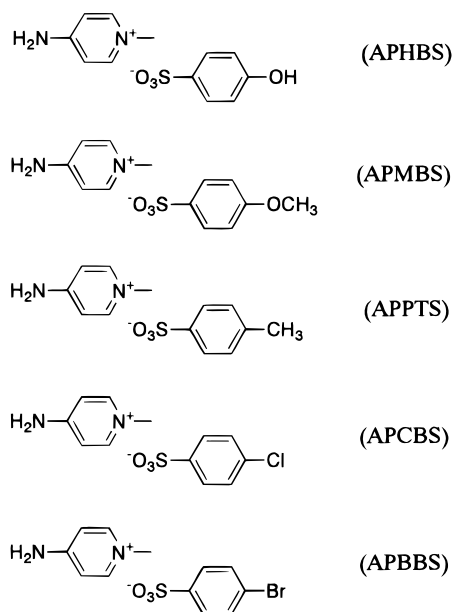

Figure 1. 4-Amino-1-methylpyridinium benzenesulfonate salts for second-order NLO and their simple abbreviations.

semiempirical MOPAC calculation[21] and experimental hyper-Rayleigh scattering (HRS) measurement[22–24] have been previously reported together with their absorption properties.[25] Their static β values are about half to twice compared with that of *p*NA irrespective of λ_{co} shorter than 400 nm, which are substantially shorter than those of stilbazolium cations. To obtain their bulk materials, on the basis of the salt methodology, we focus on crystallization of pyridinium cations with para-substituted benzenesulfonates by quaternization reaction of pyridines with methyl esters of para-substituted benzenesulfonic acids. We have reported that among the eight salts prepared of 4-amino-1-methylpyridinium benzenesulfonate derivatives, five salts were found to be SHG active.[26] In the present contribution, we report the details of synthesis and single-crystal X-ray diffraction studies of a series of the SHG active salts. The estimation of SHG coefficients of the crystals will be discussed in relation with their crystal structures and molecular hyperpolarizabilities.

Results and Discussion

Synthesis and Crystal Growth. The chemical structures of 4-amino-1-methylpyridinium benzenesulfonate salts in this study are shown in Figure 1 together with their abbreviations. The salts were synthesized by quaternization reaction of 4-aminopyridine with methyl para-substituted benzenesulfonates. The quaternization reaction gives the corresponding salts in high yields (80−85%). The chemical structures of the salts are supported satisfactorily by the ^{1}H and ^{13}C NMR data and elemental analyses results. The synthe-

(7) Meredith, G. R. In *Nonlinear Optical Properties of Organic and Polymeric Materials*, Williams, D. J., Ed.; ACS Symp. Ser. 233; American Chemical Society: Washington, DC, 1983; p 27.

(8) (a) Japanese Patent Application 61-192404, 1986. (b) Japanese Patent 1620600, 1991. Japanese Patent 1716929, 1992.

(9) Nakanishi, H.; Matsuda, H.; Okada, S.; Kato, M. In *Mater. Res. Soc. Int. Mtg. Adv. Mater.*; Doyama, M., Somiya, S., Chang, R. P. H., Eds.; Material Research Society: Pittsburgh, 1989; Vol. I, p 97.

(10) Okada, S.; Masaki, A.; Matsuda, H.; Nakanishi, H.; Kato, M.; Muramatsu, R.; Otsuka, M. *Jpn. J. Appl. Phys.* **1990**, *29*, 1112.

(11) Okada, S.; Masaki, A.; Matsuda, H.; Nakanishi, H.; Koike, T.; Ohmi, T.; Yoshikawa, N.; Umegaki, S. *Proc. SPIE* **1990**, *1337*, 178.

(12) Sakai, K.; Yoshikawa, N.; Ohmi, T.; Koike, T.; Umegaki, S.; Okada, S.; Masaki, A.; Matsuda, H.; Nakanishi, H. *Proc. SPIE* **1990**, *1337*, 307.

(13) Marder, S. R.; Perry, J. W.; Schaefer, W. P. *Science* **1989**, *245*, 626.

(14) Marder, S. R.; Perry, J. W.; Tiemann, B. G.; Marsh, R. E.; Schaefer, W. P. *Chem. Mater.* **1990**, *2*, 685.

(15) Marder, S. R.; Perry, J. W.; Schaefer, W. P.; Tiemann, B. G.; Groves, P. C.; Perry, K. J. *Proc. SPIE* **1989**, *1147*, 108.

(16) Perry, J. W.; Marder, S. R.; Perry, K. J.; Sleva, E. T.; Yakymyshyn, C. P.; Stewart, K. R.; Boden, E. P. *Proc. SPIE* **1991**, *1560*, 302.

(17) Marder, S. R.; Perry, J. W. *Adv. Mater.* **1993**, *5*, 804.

(18) Marder, S. R.; Perry, J. W.; Yakymyshyn, C. P. *Chem. Mater.* **1994**, *6*, 1138.

(19) Duan, X.-M.; Konami, H.; Okada, S.; Oikawa, H.; Matsuda, H.; Nakanishi, H. *J. Phys. Chem.* **1996**, *100*, 17780.

(20) Duan, X.-M.; Okada, S.; Oikawa, H.; Matsuda, H.; Nakanishi, H. *Jpn. J. Appl. Phys.* **1994**, *33*, L1559.

(21) Stewart, J. J. P. *MOPAC 93*; Fujitsu Limited: Tokyo, 1993.

(22) Clays, K.; Persoon, A. *Phys. Rev. Lett.* **1991**, *66*, 2980.

(23) Clays, K.; Persoon A. *Rev. Sci. Instrum.* **1992**, *63*, 3285.

(24) Duan, X.-M.; Okada, S.; Nakanishi, H.; Watanabe, A.; Matsuda, M.; Clays, K.; Persoon, A.; Matsuda, H. *Proc. SPIE* **1994**, *2143*, 41.

(25) Anwar; Duan, X.-M.; Komatsu, K.; Okada, S.; Oikawa, H.; Matsuda, H.; Nakanishi, H. *Chem. Lett.* **1997**, 247.

(26) Anwar; Duan, X.-M.; Komatsu, K.; Okada, S.; Oikawa, H.; Matsuda, H.; Nakanishi, H. *Nonlinear Opt.* **1999**, *22*, 251.

Table 1. X-ray Crystallographic Data for 4-Amino-1-methylpyridinium Benzenesulfonates

|	APHBS	APMBS	APPTS	APCBS	APBBS
formula	$C_{12}H_{14}O_4N_2S$	$C_{13}H_{16}O_4N_2S$	$C_{13}H_{16}O_3N_2S$	$C_{12}H_{13}O_3N_2SCl$	$C_{12}H_{13}O_3N_2SBr$
MW	282.30	296.40	280.40	300.80	245.20
crystal system	triclinic	monoclinic	monoclinic	monoclinic	monoclinic
space group	$P1$	$P2_1$	$P2_1$	Cc	Cc
a (Å)	6.845(3)	8.218(4)	7.891(2)	7.786(3)	7.909(3)
b (Å)	7.152(4)	10.886(4)	11.494(3)	12.126(3)	12.137(5)
c (Å)	8.095(2)	7.926(7)	7.781(2)	14.759(7)	14.760(7)
α (deg)	65.08(3)	90	90	90	90
β (deg)	83.69(4)	96.97(6)	102.20(2)	95.26(4)	93.93(3)
γ (deg)	66.16(5)	90	90	90	90
V (Å^3)	327.9(4)	703.9(8)	689.8(2)	1387.5(1)	1413.4(1)
Z	1	2	2	4	4
D_{cal} (g cm^{-3})	1.429	1.400	1.350	1.440	1.622
crystal size(mm)	0.35	0.35	0.30	0.30	0.40
	0.30	0.30	0.35	0.30	0.35
	0.20	0.20	0.20	0.20	0.30
crystal color	colorless	colorless	colorless	colorless	colorless
μ (cm^{-1})	2.46	2.33	2.29	4.21	3.24
index ranges	$-8 < h < 8$	$0 < h < 10$	$0 < h < 10$	$0 < h < 19$	$0 < h < 19$
	$0 < k < 9$	$-4 < k < 0$	$0 < k < 10$	$-15 < k < 0$	$-15 < k < 0$
	$-9 < l < 10$	$0 < l < 10$	$0 < l < 10$	$-10 < l < 10$	$-10 < l < 10$
refl measd	1677	940	1836	1791	1825
independent refl	1491	883	1664	1561	1582
observed refl	1446	829	1191	1392	1376
no. of paramtrs	183	182	226	172	172
R (all data)	0.034	0.045	0.043	0.048	0.048
max shift/esd	0.31	2.35	1.17	0.46	0.43
mean shift/esd	0.03	0.27	0.11	0.01	0.04
max diff. peak	2.27	18.61	0.23	0.23	0.37
min diff. peak	-1.87	-3.96	-0.21	-0.31	-0.36

sized salts are chemically stable and melt at temperature in the range from 144 °C for APHBS to 200 °C for APBBS without decomposition. Yields, melting points, NMR data, and elemental analyses of the salts are presented in Experimental Section.

Interestingly, single crystals suitable for X-ray diffraction studies were easily grown in methanol solution by slow evaporation. The single crystals were obtained in 3−4 weeks. Typical crystal sizes are $2 \times 2 \times 1$ mm which is indicative of good growth abilities for 4-amino-1-methylpyridinium benzenesulfonates. This ability is needed to grow large crystals for practical NLO applications.

All the crystals are naturally transparent. Their electronic absorption maxima and absorption cutoff wavelengths are at 270 and 340 nm, respectively, and there is no absorption in visible region. Typical absorption properties of the crystals are representatively shown for APHBS in Figure 2.

Molecular Geometry. The single-crystal X-ray diffraction analyses were carried out for the prepared crystals. In the structure refinement, the molecular models reached convergence with R values in range of 0.034−0.048, indicating that satisfactory complete analyses were achieved. Important details of crystal data, data collections, structure solutions, and refinements are given in Table 1. For non-hydrogen atoms, refined atomic coordinates and equivalent isotropic displacement parameters are given in Table 2. General views of the structures studied are shown in Figure 3 with the atomic numbering scheme employed.

Molecular geometry parameters of the salts studied are not exceptional. In all cases, both the 4-amino-1-methylpyridinium cation and para-substituted benzenesulfonate anions are virtually planar with normal bond lengths and bond angles as expected for aromatic compounds. In the five crystals, the bond lengths and
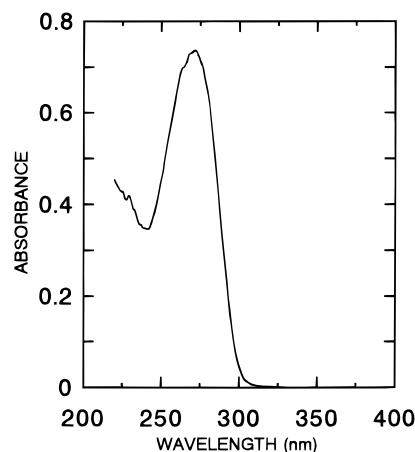
Figure 2. UV−visible spectrum of APHBS powder crystal.

bond angles of the corresponding position around 4-amino-1-methylpyridinium cation and benzenesulfonate counteranions are almost unchanged except for C(4)−X distance, where X denotes the substituent's atom attached to the aromatic ring, which must be due to the different atomic radii of X. In comparison with other crystal structures, the bond lengths and angles related to *p*-toluenesulfonate anion of APPTS were observed to be similar to those in crystals previously reported such as DAST[13] and MC−PTS.[10] We note that in the pyridinium ring, the C(8)−C(9) and C(11)−C(12) distances are equal to 1.351 Å on average and C(9)−C(10) and C(10)−C(11) are equal to 1.415 Å on average. This indicates that the double bonds are localized in the C(8)−C(9) and C(11)−C(12) bonds due to quinoidal resonance in the pyridinium ring. The similar quinoid features were also observed in X-ray diffraction studies of Lesley et al.[27] for the molecular geometry of 4-(dimethylamino)pyridinium derivatives.

Table 2. Fractional Atomic Coordinates and Equivalent Isotropic Displacement Parameters

		x/a	y/b	z/c	$U_{eq}{}^a$		x/a	y/b	z/c	$U_{eq}{}^a$
APHBS	S(1)	1.0390(0)	1.0420(0)	−0.0650(0)	419	O(4)	0.6872(7)	0.5636(4)	0.5989(2)	652
	O(1)	0.9648(9)	1.0187(8)	−0.2134(2)	579	C(7)	0.3132(6)	1.4673(1)	−0.0840(9)	664
	O(2)	0.9422(9)	1.2774(3)	−0.0860(5)	557	N(1)	0.3679(1)	1.3696(2)	0.1144(3)	486
	O(3)	1.2719(1)	0.9471(4)	−0.0353(4)	617	C(8)	0.2423(3)	1.2816(2)	0.2347(9)	533
	C(1)	0.9452(9)	0.8895(2)	0.1368(5)	383	C(9)	0.2916(8)	1.1855(1)	0.4178(7)	543
	C(2)	0.7538(6)	0.8690(1)	0.1266(1)	453	C(10)	0.4790(2)	1.1755(1)	0.4855(2)	494
	C(3)	0.6721(2)	0.7596(1)	0.2822(8)	474	C(11)	0.6063(1)	1.2696(2)	0.3569(1)	541
	C(4)	0.7783(4)	0.6682(4)	0.4507(1)	436	C(12)	0.5465(2)	1.3642(3)	0.1762(5)	536
	C(5)	0.9711(3)	0.6880(6)	0.4628(7)	500	N(2)	0.5365(7)	1.0793(3)	0.6646(3)	667
	C(6)	1.0524(8)	0.7996(1)	0.3058(6)	476					
APMBS	S(1)	0.7182(5)	0.1770(0)	0.4933(5)	440	O(4)	0.2781(3)	0.0020(2)	−0.1039(3)	731
	O(1)	0.7483(3)	0.3064(2)	0.4746(3)	590	C(7)	0.1952(4)	0.2823(3)	0.3782(4)	710
	O(2)	0.8648(3)	0.1036(2)	0.4824(3)	500	N(1)	0.1441(3)	0.3223(2)	0.2014(3)	473
	O(3)	0.6449(3)	0.1451(3)	0.6420(3)	501	C(8)	0.0225(4)	0.2565(2)	0.1070(4)	602
	C(1)	0.5832(3)	0.1310(2)	0.3104(3)	420	C(9)	−0.0262(4)	0.2860(2)	−0.0589(4)	510
	C(2)	0.5002(3)	0.0199(2)	0.3174(4)	420	C(10)	0.0439(4)	0.3838(2)	−0.1341(4)	480
	C(3)	0.4004(4)	−0.0222(2)	0.1730(4)	510	C(11)	0.1729(4)	0.4499(2)	−0.0344(4)	524
	C(4)	0.3844(3)	0.0528(2)	0.0282(4)	460	C(12)	0.2171(4)	0.4171(2)	0.1283(4)	583
	C(5)	0.4652(3)	0.1643(3)	0.0211(3)	450	N(2)	−0.0034(4)	0.4237(2)	−0.2962(4)	530
	C(6)	0.5658(3)	0.2036(2)	0.1678(3)	420	C(13)	0.2502(4)	0.0707(3)	−0.2597(4)	642
APPTS	S(1)	0.2939(0)	0.2520(0)	−0.4561(1)	520	C(7)	0.7747(3)	0.1257(3)	−0.3920(3)	630
	O(1)	0.1321(1)	0.2980(1)	−0.4268(2)	657	N(1)	0.8357(3)	0.0958(6)	−0.2018(2)	621
	O(2)	0.3692(2)	0.3088(2)	−0.5890(2)	670	C(8)	0.9581(2)	0.1601(2)	−0.0962(2)	660
	O(3)	0.2941(3)	0.1282(1)	−0.4753(2)	602	C(9)	1.0169(2)	0.1332(2)	0.0738(2)	630
	C(1)	0.4391(4)	0.2833(7)	−0.2535(9)	420	C(10)	0.9540(9)	0.0355(4)	0.1484(6)	594
	C(2)	0.5416(2)	0.3830(1)	−0.2374(2)	550	C(11)	0.8257(2)	−0.0306(2)	0.0345(2)	660
	C(3)	0.6444(4)	0.4089(3)	−0.0755(5)	620	C(12)	0.7696(2)	0.0018(2)	−0.1344(2)	672
	C(4)	0.6457(6)	0.3404(4)	0.0719(8)	571	N(2)	1.0141(2)	0.0027(2)	0.3153(2)	700
	C(5)	0.5454(6)	0.2409(3)	0.0526(9)	580	C(13)	0.7616(3)	0.3713(2)	0.2465(3)	642
	C(6)	0.4413(9)	0.2130(5)	−0.1106(7)	511					
APCBS	S(1)	0.7805(4)	0.5181(2)	0.9710(2)	501	Cl(1)	0.2340(0)	0.3341(3)	0.6710(0)	592
	O(1)	0.7243(0)	0.4893(6)	1.0590(4)	774	C(7)	0.7617(9)	0.1594(8)	0.9399(5)	655
	O(2)	0.9323(7)	0.4566(4)	0.9484(4)	540	N(1)	0.7281(8)	0.1710(5)	0.8399(4)	503
	O(3)	0.8035(9)	0.6357(4)	0.9569(4)	700	C(8)	0.6112(9)	0.1034(6)	0.7936(5)	564
	C(1)	0.6113(9)	0.4732(6)	0.8879(5)	451	C(9)	0.5754(9)	0.1110(6)	0.7023(5)	484
	C(2)	0.4943(9)	0.3973(6)	0.9106(5)	520	C(10)	0.6657(9)	0.1906(6)	0.6524(5)	494
	C(3)	0.3774(9)	0.3565(7)	0.8435(5)	610	C(11)	0.7846(9)	0.2614(6)	0.7035(5)	524
	C(4)	0.3803(9)	0.3920(7)	0.7552(5)	562	C(12)	0.8118(9)	0.2488(6)	0.7942(6)	534
	C(5)	0.4940(9)	0.4702(7)	0.7312(5)	571	N(2)	0.6377(9)	0.1966(6)	0.5611(5)	594
	C(6)	0.6105(9)	0.5104(7)	0.7982(5)	520					
APBBS	S(1)	0.7115(4)	−0.0155(4)	0.1022(9)	491	Br(1)	1.2650(0)	0.1683(1)	0.4020(0)	643
	O(1)	0.5659(9)	0.0475(6)	0.1279(5)	593	C(7)	0.7388(9)	0.3403(9)	0.1406(7)	605
	O(2)	0.6885(9)	−0.1324(6)	0.1162(6)	704	N(1)	0.7734(9)	0.3304(7)	0.2394(5)	494
	O(3)	0.7652(9)	0.0120(8)	0.0135(5)	714	C(8)	0.8864(9)	0.3941(8)	0.2843(7)	524
	C(1)	0.8769(9)	0.0240(7)	0.1835(6)	474	C(9)	0.9211(9)	0.3869(7)	0.3754(7)	484
	C(2)	0.9966(9)	0.1031(7)	0.1586(6)	524	C(10)	0.8367(9)	0.3085(8)	0.4259(7)	524
	C(3)	1.1120(9)	0.1424(9)	0.2243(8)	575	C(11)	0.7210(9)	0.2384(8)	0.3758(7)	544
	C(4)	1.1102(9)	0.1061(9)	0.3127(7)	534	C(12)	0.6923(9)	0.2507(8)	0.2858(7)	544
	C(5)	0.9965(9)	0.0267(9)	0.3364(7)	615	N(2)	0.8618(9)	0.3001(8)	0.5149(6)	604
	C(6)	0.8790(9)	−0.0142(8)	0.2719(7)	534					

^{a} U_{eq} is in 10^{-4} Å^2.

Although the planes of pyridinium ring and benzenesulfonate ring are nearly parallel in the five crystals, the angle between the molecular axes of pyridinium cation and benzenesulfonate counteranion vary depending on the molecular geometry. For similar substituents, the angle between the molecular axes are the same, for instance, those in APHBS and APMBS crystals are about 42.4°, and those in APCBS and APBBS crystals are about 38.4°. Meanwhile that of APPTS is 31.5°.

Microscopic NLO Properties. At the molecular state, the first hyperpolarizability (β) of 4-amino-1-methylpyridinium cation and para-substituted benzenesulfonate anions were independently evaluated. Namely, 4-amino-1-methylpyridinium iodide and sodium para-substituted benzenesulfonates were used for HRS measurement. The obtained β values at 1064 nm in methanol solution for the ionic species are summarized in Table 3 along with the λ_{max} and λ_{co} values. For comparison, those for 2-methyl-4-nitroaniline (MNA) are also added in this table. The β values and the absorption properties of several of these ionic species have been reported previously.[25,28] The β values of the ionic species are less than half of that of MNA. However, it should be stressed that they have no absorption in visible region and their λ_{co} is shorter than that of MNA of more than 100 nm. Especially for the para-substituted benzenesulfonate anions, electron-donor substituents (OH,

(27) Lesley, M. J. G.; Woodward, A.; Taylor, N. J.; Marder, T. B.; Gazenobe, I.; Ledoux, I.; Zyss, J.; Thornton, A.; Bruce, D. W.; Kakkar, A. K. *Chem. Mater.* **1998**, *10*, 1355.

(28) (a) Duan, X.-M.; Okada, S.; Oikawa, H.; Matsuda, H.; Nakanishi, H. *Mol. Cryst. Liq. Cryst.* **1995**, *267*, 89. (b) Anwar; Komatsu, K.; Okada, S.; Oikawa, H.; Matsuda, H.; Nakanishi, H. *Proc. SPIE* **1999**, *3796*, 219.
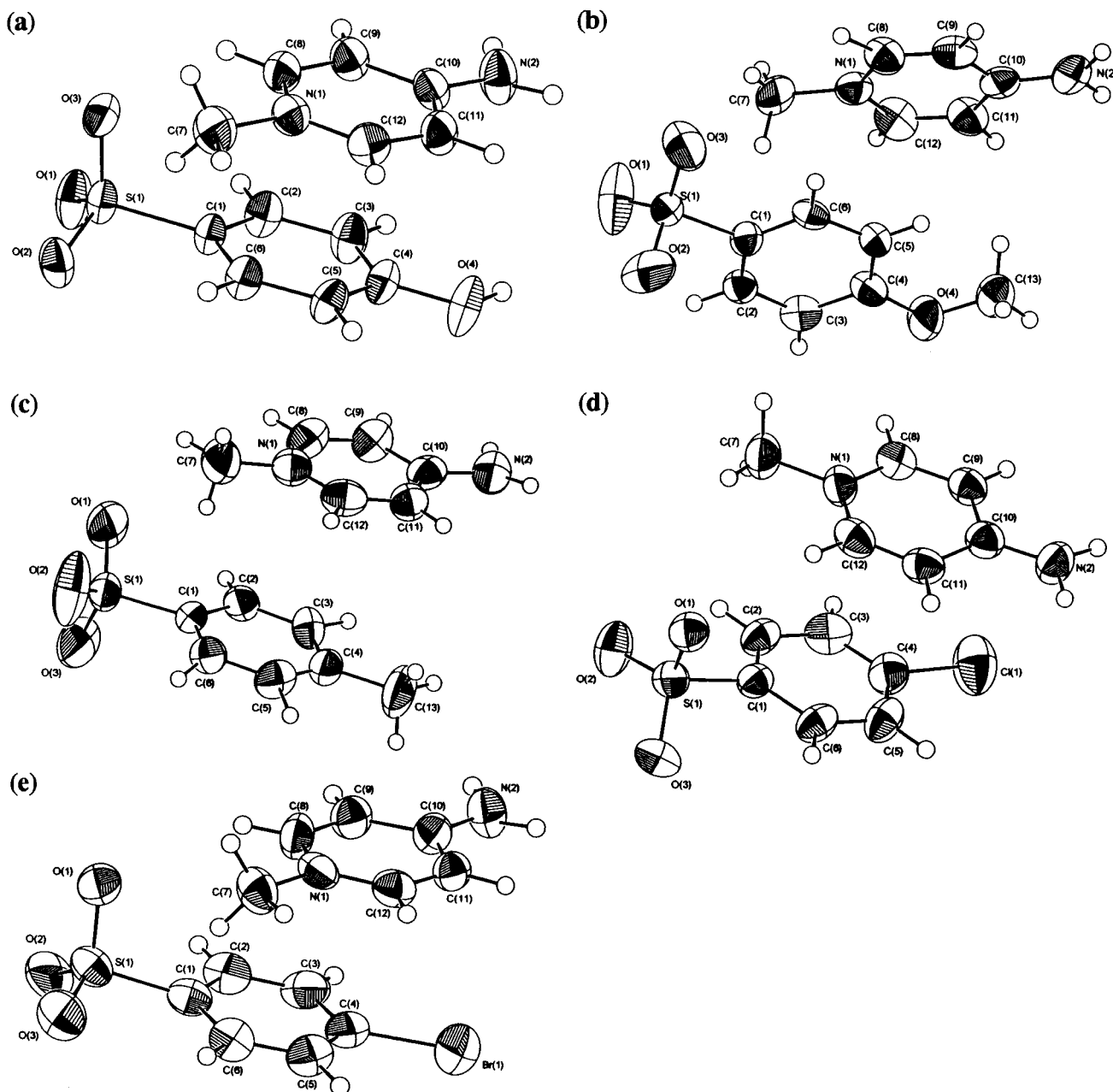
(a)

(b)

(c)

(d)

(e)

Figure 3. Molecular geometries of (a) APHBS, (b) APMBS (c) APPTS, (d) APCBS, and (e) APBBS with 50% probability ellipsiods.

and OCH₃, CH₃) tend to give larger β value than other substituents (Cl and Br). Although this seems to be inconsistent with the role of sulfonate anion being an electron donor, but in fact this is due to the methanol solvent effect on β, which is discussed elsewhere in detail.[29]

Crystal Packing Analysis and Estimation of Macroscopic NLO Susceptibility. Crystal packing diagrams for the structures of crystals studied are presented in Figures 4–6. In these figures, the relatively weak intermolecular hydrogen-bond interactions between amino-hydrogen atoms and the adjacent sulfonate-oxygen atoms are shown by dotted lines. The closest intermolecular distances between amino-hydrogen and sulfonate-oxygen [H···O] and those between amino-nitrogen and sulfonate-oxygen [N···O] listed in

Table 4 are in the range of 1.85–2.05 Å and 2.85–3.00 Å, respectively, while the angles ∠N—H···O are in the range of 153–171° which satisfies the criteria for the existence of intermolecular N—H···O hydrogen bonds.[30] The hydrogen bonds connect a cation of an ion pair to the adjacent anion of another ion pair. Therefore, the hydrogen-bonding network forms infinite ion-pair arrays. In several cases, specific intermolecular hydrogen-bonding networks have been used as a steering force for structure acentricity in crystal engineering, particularly for second-order nonlinear optics in works of Etter's group[31,32] and Günter's group.[33–35] In the present crystals, the infinite hydrogen bonds which are perpen-

(29) Anwar; Duan, X.-M.; Okada, S.; Oikawa, H.; Matsuda, H.; Nakanishi, H. *Phys. Chem. Chem. Phys.*, submitted for publication.
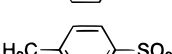
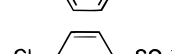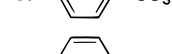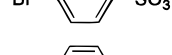(30) Zefirov, Y. V. *Kristallografiya* **1998**, *43*, 313.
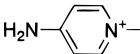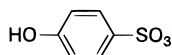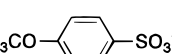
(31) Panunto, T. W.; Urbanczyk-Lipkowska, Z.; Johnson, R.; Etter, M. C. *J. Am. Chem. Soc.* **1987**, *109*, 7786.

(32) Etter, M. C.; Baures, P. W. *J. Am. Chem. Soc.* **1988**, *110*, 639.

(33) Pan, F.; Wong, M. S.; Bosshard, C.; Günter, P.; Gramlich, V. *Adv. Mater. Opt. Electron.* **1996**, *6*, 261.

Table 3. Absorption Properties and First Hyperpolarizability of 4-Amino-1-methylpyridinium and Para-Substituted Benzenesulfonates along with Those of MNA

Molecule	$\lambda_{max}{}^a$	$\lambda_{co}{}^a$	$\beta^{a,b}$	Reference
H_2N—〈 〉—N^+—	270	315	12	25
HO—〈 〉—SO_3^-	232	314	17	35
H_3CO—〈 〉—SO_3^-	232	324	19	This work
H_3C—〈 〉—SO_3^-	222	280	22	20
Cl—〈 〉—SO_3^-	226	298	10	35
Br—〈 〉—SO_3^-	230	312	11	This work
H_2N—〈 〉—NO_2	372	475	42	40

[a] The absorption data are in nanometers for their methanol solution. [b] The β value is in 10^{-30} esu measured at 1064 nm.
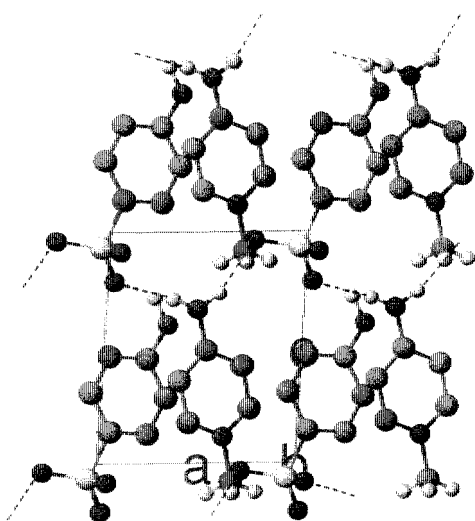
Figure 4. Crystal packing diagram for APHBS down the crystallographic *a* axis. Protons on aromatic rings are omitted.

dicular to polar orientation of the ionic species play an important role in construction of the noncentrosymmetric crystal structures. The hydrogen-bonding networks seem to tailor the molecular dipoles of the ionic species in similar direction. The presence of the hydrogen bond, beside the Coulombic interactions between the ionic species, helps in building up stable structures, and is also one of the favorable factor to have high melting point and to grow single crystals with relative ease.

Since the arrangements of molecular dipoles in the noncentrosymmetric space groups are responsible for $\chi^{(2)}$, the crystal packing analyses for the five structures are important for understanding their second-order NLO properties in the crystalline state. According to our
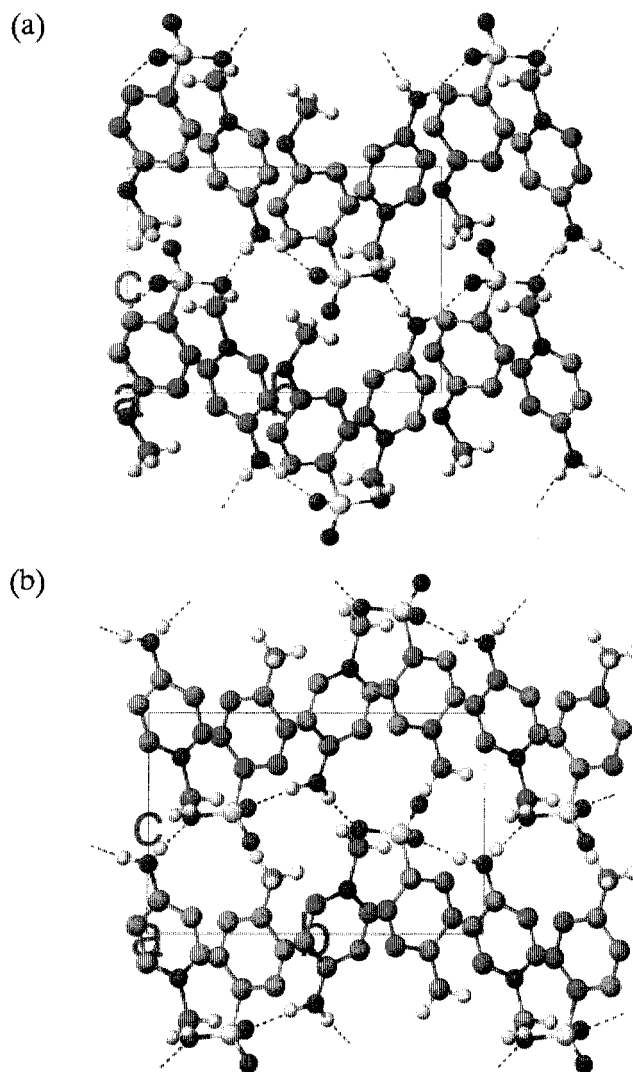
(34) Wong, M. S.; Pan, F.; Gramlich, V.; Bosshard, C.; Günter, P. *Adv. Mater.* **1997**, *9*, 554.

(35) Wong, M. S.; Pan, F.; Bosch, M.; Spreiter, R.; Bosshard, C.; Günter, P.; Gramlich, V. *J. Opt. Soc. Am. B* **1998**, *15*, 426.

Figure 5. Crystal packing diagrams for (a) APMBS and (b) APPTS down the crytallographic *a* axis. Protons on aromatic rings are omitted.

MOPAC calculations, the dipole moment vectors of 4-amino-1-methylpyridinium cation and para-substituted benzenesulfonate anions coincide with their molecular axes. That of the cation is in the direction from N(1) to N(2), and those of the anions are in the direction from S(1) to C(4).

For crystal structure of APHBS (Figure 4), the space group is triclinic *P*1 and there is one ion-pair per unit cell. This structure belongs to a 1-C_1 class symmetry, therefore this crystal has all 18 independent components of second-harmonic (*d*) or electrooptic (*r*) coefficients by Kleinman symmetry.[36] The angles between the dipole moment direction and the crystallographic *a*, *b*, and *c* axes for 4-amino-1-methylpyridinium cation are 78.7°, 86.3°, and 25.6°, respectively. Those for *p*-hydroxybenzenesulfonate anion are 57.1°, 68.8°, and 38.5°, respectively. Since both cation and anion have almost equal β values, all allowed *d* components would be sizable.

The crystal structures of APMBS and APPTS (Figure 5) belong to monoclinic space group *P*2$_1$ (2-C_2 crystal class symmetry) with monoclinic angle β of 96.97° and 102.2°, respectively. This particular structure has been

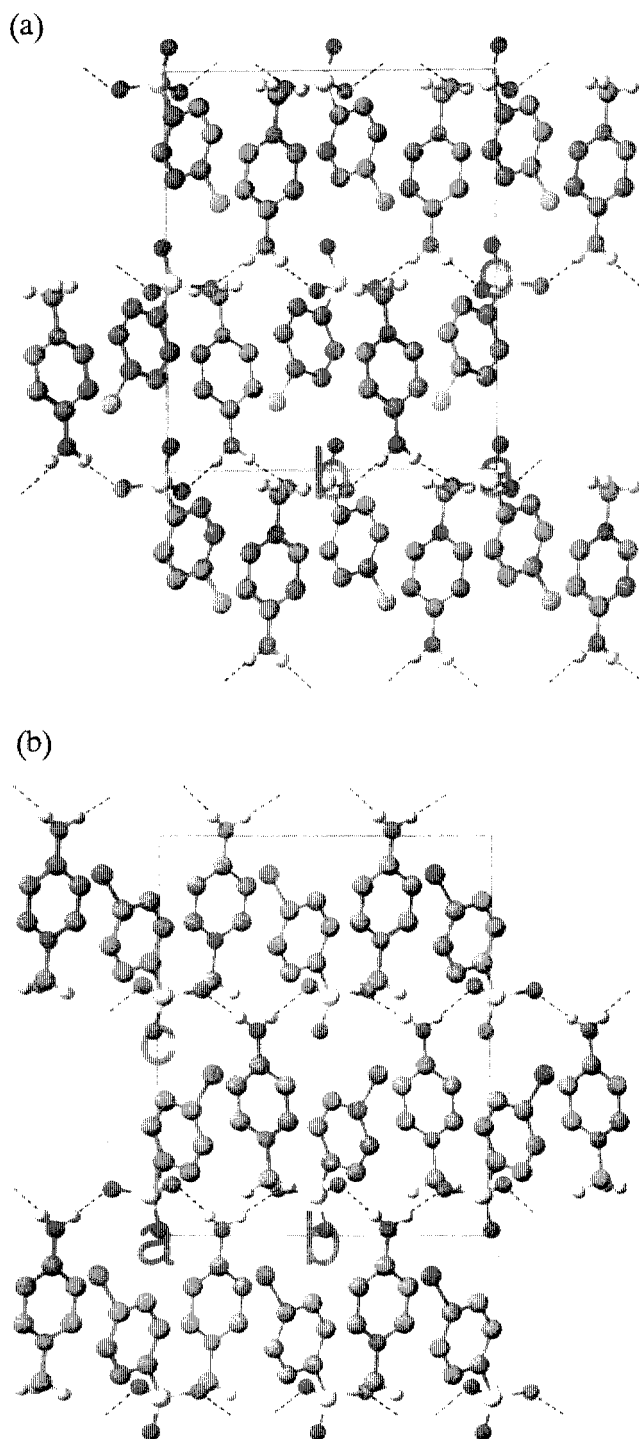(36) Kleinman, D. A. *Phys. Rev. A* **1962**, *126*, 1977.

(a)

(b)

Figure 6. Crystal packing diagram for (a) APCBS and (b) APBBS down the crytallographic *a* axis. Protons on aromatic rings are omitted.

Table 4. Hydrogen-Bond Distances (*d*, Å) and Angle (deg) Observed for 4-Amino-1-methylpyridinium Benzenesulfonate Crystals Investigated

crystal	$d(O\cdots H)$	$d(O\cdots N)$	$\angle N-H\cdots O$
APHBS	2.04, 2.05	2.93, 3.00	167.8, 152.6
APMBS	1.81, 1.91	2.78, 2.86	170.3, 170.6
APPTS	1.85, 1.77	2.83, 2.85	167.1, 165.7
APCBS	1.93, 1.96	2.88, 2.92	168.5, 173.8
APBBS	1.96, 1.98	2.91, 2.92	160.8, 170.0

described in great details for well-known methyl 2-((2,4-dinitrophenyl)amino)propanoate (MAP)[37] and *N*-(4-nitrophenyl)-L-prolinol (NPP)[38] by Zyss et al. In their unit

cells, there are two ion pairs which are interchanged by a 2-fold rotation around the unique polar *b* axis. The nonvanishing components of second-harmonic coefficients, d_{IJK}, allowed by the 2-C_2 symmetry and Kleinman symmetry are d_{14}, d_{16}, d_{21}, d_{22}, and d_{23}. The angle of molecular dipoles of 4-amino-1-methylpyridinium cation and *p*-methoxybenzenesulfonate anion with respect to the crystallographic polar axis in APMBS are approximately 75° and 71°, while those of 4-amino-1-methylpyridinium cation and *p*-toluenesulfonate anion in APPTS are approximately 60° and 72°. Among the nonvanishing *d* components, the diagonal d_{22} and non-diagonal d_{23} components would be optimum in these crystals.

The crystal structures of APCBS and APBBS (Figure 6) belong to monoclinic space group *Cc* (class 4-C_{1h} symmetry). This crystal class symmetry has also been described in detail by Levine et al.[39] for MNA. In the unit cells of the two crystals, there are four ion pairs which are glided in planes perpendicular to the crystallographic *b* axis. By the 4-C_{1h} symmetry and the Kleinman symmetry for this particular arrangements, there are seven nonvanishing components of d_{IJK}, i.e., d_{11}, d_{12}, d_{13}, d_{15}, d_{24}, d_{26}, and d_{33}. The angle of molecular dipoles of 4-amino-1-methylpyridinium cation and its counteranion in APCBS to polar *c* axis are approximately 11° and 48°, while those of 4-amino-1-methyl-pyridinium cation and its counteranion in APBBS are approximately 12° and 48°. Among the nonvanishing *d* components in these crystals, the diagonal d_{33} and nondiagonal d_{24} components would be optimum.

The relationship between microscopic and macroscopic second-order optical nonlinearities, with the assumption of no any intermolecular interactions, *d* coefficients are calculated as[40]

$$d_{IJK} = Nf_I^{2\omega} f_J^{\omega} f_K^{\omega} \sum \cos\theta(I,i) \cos\theta(K,k) \cos\theta(J,j) \beta_{ijk} \quad (1)$$

where N is the number of chromophores in a unit volume, and $f_I^{2\omega}$, f_J^{ω}, and f_K^{ω} are Lorentz's local field factors. The summation involves over all molecules in a unit cell, and cosine product terms represent the effective β value to the optical frame. In the case of "push–pull" compounds such as 4-amino-1-methylpyridinium and para-substituted benzenesulfonates, only the component of β_{ijk} along the charge-transfer axis *z* of the molecule (β_{zzz}) is large and consideration on this contribution to the corresponding crystalline second-order nonlinear coefficient is enough to be taken into account. Thus, the diagonal and nondiagonal *d* components can be written as $d_{ZZZ} = Nf_Z^{2\omega}f_Z^{\omega}f_Z^{\omega} \sum\cos^3\theta_i\beta_{zzz}$ and $d_{XZZ} = Nf_X^{2\omega}f_Z^{\omega}f_Z^{\omega} \sum\cos\theta_i\sin^2\theta_i\beta_{zzz}$, respectively. Angles θ in these equations are shown in Figure 7 using APBBS as an example, where θ_c and θ_a are for cation and anion, respectively. In the case of APHBS, diagonal *d* component is optimized when the optical *Z* axis is parallel to one of the ionic molecular axis.

(37) Oudar, J. L.; Zyss, J. *Phys. Rev. A* **1982**, *26*, 2016.

(38) Zyss, J.; Nicoud, J. F.; Coquillay, M. *J. Chem. Phys.* **1984**, *81*, 4160.

(39) Levine, B. F.; Bethea, C. G.; Thurmond, C. D.; Lynch, R. T.; Bernstein, J. L. *J. Appl. Phys.* **1979**, *50*, 2523.

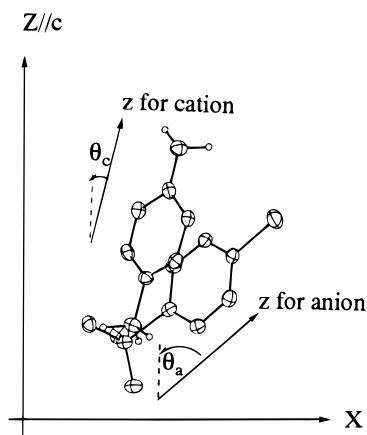(40) Zyss, J.; Oudar, J. L. *Phys. Rev. A* **1982**, *26*, 2028.

Figure 7. ORTEP view of APBBS showing the angles $\theta_c = 12°$ and $\theta_a = 48°$ between the optical Z axis and molecular charge-transfer axis z for cation and anion, respectively. The optical Z axis was set to coincide with the crystallographic polar c axis.

Table 5. Absorption Cutoff Wavelength (λ_{co}), Space Group, Estimated d Coefficients Using the Oriented-Gas Model and Related Parameters of the Crystals Investigated

crystal	λ_{co} (nm)	space group	N^a (10^{21} mol·cm^{-3})	θ_c, θ_a	$d_{zzz}{}^b$	$d_{zxx}{}^b$
APHBS	340	$P1$	3.05	0°, 10°	148	3
APMBS	340	$P2_1$	2.80	75°, 71°	4	14
APPTS	340	$P2_1$	2.90	60°, 72°	10	18
APCBS	340	Cc	2.88	11°, 48°	70	7
APBBS	340	Cc	2.83	12°, 48°	70	7
MNA[39]	475	Cc	5.85	21°	583 (250)	14 (27)

Using this oriented-gas model, we estimated their nonvanishing coefficients to screen the most potential NLO crystals among the prepared crystals in simple comparison with MNA. In this estimation, we employed the measured β in methanolic solution at 1064 nm wavelength (Table 3). Local field factors for present crystals were referred to those of 3-methoxy-4-hydroxy-benzaldehyde (MHBA)[41] crystal, because MHBA belongs to monoclinic space group $P2_1$ and has an absorption cutoff around 370 nm which is close to that of the crystals in this study. For MNA, refractive indices in the literature; i.e., $n_{2\omega}$ of 2.2 and n_ω of 1.8 were used to calculated the local field factors. As a result, the diagonal d component of APHBS was estimated to be about one-third, while those of other four crystals are less than one-sixth, smaller than that of MNA. For the nondiagonal d components of the other four crystals are about equal to double that of MNA as listed in Table 5. The relatively smaller diagonal and nondiagonal d components in the present crystals other than that of MNA are mainly due to much smaller β values of 4-amino-1-methylpyridinium cation and para-substituted benzenesulfonate anions compared with that of MNA. However, in several cases, their molecular alignments are close to the optimization of d components. For instance, the estimated d_{XZZ} of APPTS is about 82% of the optimum situation, i.e., when θ is equal to 54.74° for both ionic species.[38]

The estimated d components may not match well with the experimental values, since the estimated d_{11} com-

(41) Tao, X. T.; Yuan, D. R.; Zhang, N.; Jiang, M. H.; Shao, Z. S. *Appl. Phys. Lett.* **1992**, *60*, 1415.

ponent of MNA was estimated to be 582 pm/V which is greatly overestimated when compared with the experimental value of 250 pm/V.[39] This can be understood by considering that environment of a molecule is different between in solution and in a crystal. As the result, β value of the molecule may be different. However, by this relative comparison, we may expect to select the most potential NLO crystals among the crystals in this study.

Conclusions

The crystals of a series of 4-amino-1-methylpyridinium para-substituted benzenesulfonate salts were found to be new second-order NLO materials having a short cutoff wavelength within UV region. We may note that the intermolecular hydrogen-bonding network formed between amino-hydrogen atoms of a cation of an ion pair and sulfonate-oxygen atoms of adjacent anions of another ion pair are interesting features and play an important role to achieve noncentrosymmetric structures in the present crystals.

Crystal of APHBS provides good molecular arrangement to optimize a diagonal d component, while APPTS and APMBS were found to give crystals with large nondiagonal d components. They may be a new series of useful colorless crystals for second-order NLO applications such as electrooptic or frequency doubler of conventional diode lasers. The next step of our studies will be the growth of larger crystals for optical measurements to determine their d or r components.

Experimental Section

Starting Materials and Equipments. All starting compounds were purchased from Aldrich or Kanto Chemical and used without further purifications. The nuclear magnetic resonance spectra were obtained on a JEOL JNM-LA400 spectrometer operating in the Fourier transform mode at 400 MHz. All the spectra were recorded in methanol-d_4 solution, and the proton chemical shifts were referred to the internal standard tetramethylsilane (TMS). The UV−visible spectra were recorded on Jasco V-570 spectrophotometer. For solution samples, the absorption maximum wavelengths (λ_{max}) and absorption cutoff wavelengths (λ_{co}) of the ionic species in methanol were measured in concentrations of 4×10^{-4} and 1×10^{-2} M, respectively. For crystalline samples, crushed single crystals with potassium bromide (KBr) by a ratio of 1:100 in weight were prepared and their spectra were measured by the diffuse reflection method using the pure KBr sample as a reference. Melting points were determined without correction using Yanaco MP-500 for powder crystals sandwiched between microcover glasses. Elemental analyses were obtained from ICRS, Tohoku University. The β value of 4-aminopyridinium cation as well as those of para-substituted benzenesulfonate anions were determined by the HRS technique using a Q-switched Nd:YAG laser at 1064-nm wavelength with 10-ns pulse width. The experimental setup and determination method of β value have been previously described in detail.[24]

Synthesis of 4-Amino-1-methylpyridinium Benzenesulfonate Salts. To solutions of 10 mmol of para-substituted benzenesulfonyl chlorides in 100 mL of methanol was added 10 mL of sodium methoxide meth-

anol solution (1 mM). The mixtures were stirred for 2 h at room temperature. After the solvent was evaporated in a vacuum, the residue was dissolved in ether and was filtered to remove sodium chloride. After the ether was removed from the filtrate by evaporation, the corresponding methyl para-substituted benzenesulfonate was obtained. These methyl esters (5 mmol) were dissolved in 50 mL of methanol. To these solutions was added an equimolar of 4-aminopyridine methanol solution. After the solution was stirred gently for a few days, precipitated solids of desired salts were filtered off. After the salts were dried in a vacuum and recrystallized from methanol, the pure salts were obtained.

1-Amino-1-methylpyridinium *p*-hydroxybenzenesulfonate, **APHBS**: Yield 86%; mp 144–146 °C; ^{1}H NMR δ (ppm) J (Hz) 3.79 (s, 3H, N–CH_3), 6.70 (d, 2H, J = 8.8, H$_{aromatic}$), 7.00 (d, 2H, J = 7.6, H$_{aromatic}$), 7.54 (d, 2H, J = 8.8, H$_{aromatic}$), 7.87 (d, 2H, J = 7.6, H$_{aromatic}$); ^{13}C NMR δ (ppm) 45.1 (N–CH$_3$), 110.7, 115.7, 128.7, 137.3, 144.6, 160.3, 160.5 (C$_{aromatic}$). Anal. Calcd for C$_{12}$H$_{14}$O$_4$N$_2$S (282.32): C 51.05, H 5.00, N 9.91. Found: C 51.26, H 5.00, N 9.81. 4-Amino-1-methylpyridinium *p*-methoxybenzenesulfonate, **APMBS**: Yield 84%; mp 189–191 °C; ^{1}H NMR δ (ppm), J (Hz) 3.72 (s, 3H, O–CH_3), 3.79 (s, 3H, N–CH_3), 6.69 (d, 2H, J = 7.6, H$_{aromatic}$), 6.82 (d, 2H, J = 8.8, H$_{aromatic}$), 7.63 (d, 2H, J = 8.8, H$_{aromatic}$), 7.86 (d, 2H, J = 7.6, H$_{aromatic}$); ^{13}C NMR δ (ppm) 45.1 (N–CH$_3$), 55.9 (O–CH3), 110.7, 114.4, 128.6, 138.6, 144.7, 160.4, 162.5 (C$_{aromatic}$). Anal. Calcd for C$_{13}$H$_{16}$O$_4$N$_2$S (296.35): C 52.68, H 5.40, N 9.40. Found: C 52.67, H 5.40, N 9.46.

4-Amino-1-methylpyridinium *p*-toluenesulfonate, **APPTS**: Yield 90%; mp 184–186 °C; ^{1}H NMR δ (ppm) J (Hz) 2.56 (s, 3H, CH_3–C$_6$H$_4$), 3.79 (s, 3H, N–CH_3), 6.69 (d, 2H, J = 7.6, H$_{aromatic}$), 7.11 (d, 2H, J = 8.3, H$_{aromatic}$), 7.58 (d, 2H, J = 8.3, H$_{aromatic}$), 7.86 (d, 2H, J = 7.6, H$_{aromatic}$); ^{13}CNMR δ (ppm) 21.3 (CH$_3$), 45.1 (N–CH$_3$), 110.7, 126.9, 129.8, 141.7, 143.6, 144.7, 160.4 (C$_{aromatic}$). Anal. Calcd for C$_{13}$H$_{16}$O$_3$N$_2$S (280.35): C 55.69, H 5.75, N 9.99. Found: C 55.76, H 5.87, N 10.00.

4-Amino-1-methylpyridinium *p*-chlorobenzenesulfonate, **APCBS**: Yield 88%; mp 195–197 °C; ^{1}H NMR δ (ppm) J (Hz) 3.79 (s, 3H, N–CH_3), 6.69 (d, 2H, J = 7.8, H$_{aromatic}$), 7.32 (d, 2H, J = 8.6, H$_{aromatic}$), 7.68 (d, 2H, J = 8.8, H$_{aromatic}$), 7.88 (d, 2H, J = 7.6, H$_{aromatic}$); ^{13}C NMR δ (ppm) 45.1 (N–CH_3), 110.7, 128.6, 129.4, 137.1, 144.7, 145.3, 160.4 (C$_{aromatic}$). Anal. Calcd for C$_{12}$H$_{13}$O$_3$N$_2$SCl (300.76): C 47.92, H 4.36, N 9.19. Found: C 47.79, H 4.34, N 9.32.

4-Amino-1-methylpyridinium *p*-bromobenzenesulfonate, **APBBS**: Yield 88%; mp 198–200 °C; ^{1}H NMR δ (ppm) J (Hz) 3.79 (s, 3H, N–CH_3), 6.69 (d, 2H, J = 7.6, H$_{aromatic}$), 7.47 (d, 2H, J = 8.6, H$_{aromatic}$), 7.61 (d, 2H, J = 8.6, H$_{aromatic}$), 7.88 (d, 2H, J = 7.6, H$_{aromatic}$); ^{13}C NMR

δ(ppm) 45.1 (N–CH_3), 110.7, 125.3, 128.8 132.5, 144.7, 145.7, 160.4 (C$_{aromatic}$). Anal. Calcd for C$_{12}$H$_{13}$O$_3$N$_2$SBr (345.21): C 41.74, H 3.80, N 8.11. Found: C 41.85, H 3.82, N 8.01. We note that the protons of amino and hydroxy groups could not be detected in methanol-d_4.

Single crystals of the salts were obtained by slow evaporation method. In 10 mL of methanol were dissolved 1 g of the salts, and the solutions were put into crystal dishes after removing the particulates by filtration. These dishes were covered with aluminum foil and were kept in a desiccator.

X-ray Data Collection and Structure Determination. For the X-ray structure determination, the grown single crystals were cut to a proper size and mounted on glass rods with epoxy cement. Cell parameter determination and data collection were performed on a MacScience MXC-18 four-circle diffractometer using graphite-monochromated Mo Kα radiation (λ = 0.71073 Å). The crystal cell parameters were determined from the observed setting angles of 22 preliminary reflections, and data of intensities were collected by ω scan. Fluctuations of intensity were monitored for three standard reflections in every 100 reflections during the all measurements.

The crystal structures were solved by direct methods (SHELXS-86[42]) and refined by full-matrix least-squares procedures. The refinement were on F of reflections with criterion $F > 3\sigma(F)$ to minimize $\sum w(|F_o| - |F_c|)^2$, where weighting factor w was taken to be 1, F_o and F_c are the observed and calculated structure factors. A large number of variable parameters of observed reflections were converged with residual value, $R = \sum(||F_o| - |F_c||)/\sum(|F_o|)$. In all the cases, non-hydrogen atoms are refined by anisotropic displacement parameters. Hydrogen atoms were found with difference Fourier synthesis or were attached on their parent atoms with fixed bond lengths and idealized bond angles. In the crystal structure analyses, absorption corrections were not applied because the linear absorption coefficient, μ, were found to be quite small, implying that the extinction correction were negligible. All calculations were performed using Crystan-GM program[43] running on a workstation. The drawings of the molecular structures were obtained by ORTEP.

(42) Sheldrick, G. M. *SHELXS86, Program for Crystal Structure Solution*; University of Göttingen: Germany, 1986.
(43) Crystan-GM. *MAC Science Limited*, Yokohama, 1994.